Opening Four-Wave Mixing and Six-Wave Mixing Channels via Dual Electromagnetically Induced Transparency Windows

Yanpeng Zhang,* Andy W. Brown, and Min Xiao†

Department of Physics, University of Arkansas, Fayetteville, Arkansas 72701, USA

(Received 25 November 2006; published 18 September 2007)

Highly efficient four-wave mixing (FWM) and six-wave mixing (SWM) processes can coexist in a four-level Y-type atomic system due to atomic coherence. The simultaneously opened dual electromagnetically induced transparency windows in this four-level atomic system allow observation of these two nonlinear optical processes at the same time, which enables detailed studies of the interplay between the FWM and SWM processes. Three-photon and five-photon destructive interferences are also observed.

DOI: 10.1103/PhysRevLett.99.123603 PACS numbers: 42.50.Gy, 32.80.Qk, 42.65.−k

Enhanced four-wave mixing (FWM) processes due to atomic coherence have been experimentally demonstrated in several multilevel atomic systems [1–5]. The keys to such enhanced nonlinear optical processes include the enhanced nonlinear susceptibility due to the induced atomic coherence and slowed laser beam propagation in the atomic medium, as well as greatly reduced linear absorption of the generated optical field due to electromagnetically induced transparency (EIT) [6,7]. Recently, the generation of six-wave mixing (SWM) has been reported in a closed-cycle N-type system in a cold atomic sample [8]. On the other hand, two-photon and three-photon destructive interferences have also been studied in various four-level Y-type [9], N-type [10], and double-Λ-type [2,5] atomic systems. These multiphoton interferences and light-induced atomic coherence are very important in nonlinear wave-mixing processes and might be used to open certain nonlinear optical processes in multilevel atomic systems that are otherwise closed due to high absorption [11]. Recently, there has been some theoretical interest in generating efficient $\chi^{(5)}$ processes in multilevel atomic systems for 3-qubit quantum computation [12] and liquid light condensate [13].

In this Letter, we report our experimental demonstration of generating highly efficient FWM and SWM processes simultaneously in an open-cycle Y-type atomic system, in which the dual-EIT windows are used to transmit the generated FWM and SWM signals, respectively. Several features in this work are distinctly different and advantageous over the previously reported SWM processes [8,14]. First, FWM and SWM processes can be observed simultaneously in this open-cycle Y-type system, which is not the case in the closed-cycle N-type system [8]. Such coexistence of FWM and SWM processes allows us to investigate the interplay between these two interesting nonlinear optical effects, and to obtain the beat signal between them to get the $\chi^{(5)}$ coefficient. Second, the generated FWM and SWM signals fall into two separate EIT windows in this four-level dual-EIT system, so the linear absorptions for the generated FWM and SWM signals are both greatly suppressed. By individually controlling (or tuning) the EIT windows, the generated FWM and SWM signals can be clearly separated and distinguished or pulled together (by frequency detunings) to observe interferences between them. Third, since the amplitude of the FWM signal can be controlled by the coupling beam (via dressed states), the relative strengths of the FWM and SWM can be adjusted easily. So, the SWM signal can be made to be in the same order as the FWM signal. Fourth, multiphoton destructive interference effects for both FWM (three-photon interference) and SWM (five-photon interference) are clearly observed in the experiment. Although double-resonance [9] and triple-resonance [10,15] EIT spectroscopies have been reported previously by detecting fluorescence, the current method is a coherent phenomenon. Finally, by designing the propagation directions of the (pump, coupling, and probe) laser beams, we can achieve Doppler-free configurations [7] for all the EIT subsystems in this Y-type atomic system. This makes the FWM and SWM processes very efficient even with relatively weak cw laser beams in an atomic vapor cell.

To the best of our knowledge, such a phenomenon of coexisting FWM and SWM channels via dual-EIT windows in multilevel atomic systems has not been reported, either experimentally or theoretically, in the literature. This specially designed experimental scheme to simultaneously generate different nonlinear wave-mixing processes opens a new research frontier in manipulating higher-order nonlinear optical processes with induced atomic coherence and quantum interference.

For a simple four-level Y-type atomic system as shown in Fig. 1(b), if two strong laser beams drive the two upper transitions ($|1\rangle$ to $|2\rangle$ and $|1\rangle$ to $|3\rangle$, respectively) and a weak laser beam probes the lower transition ($|0\rangle$ to $|1\rangle$), two ladder-type EIT subsystems will form and two EIT windows appear [9]. Depending on the frequency detunings of the two coupling beams, these two EIT windows can either overlap or be separated in frequency on the probe beam transmission signal. Now, if two pump fields, E_3 (ω_3, $\mathbf{k}_3$, and Rabi frequency G_3) and E_3' (ω_3, $\mathbf{k}_3'$, and Rabi frequency G_3'), drive the upper transition $|1\rangle$ to $|3\rangle$ and one strong field, E_2 (ω_2, $\mathbf{k}_2$, and Rabi frequency G_2),

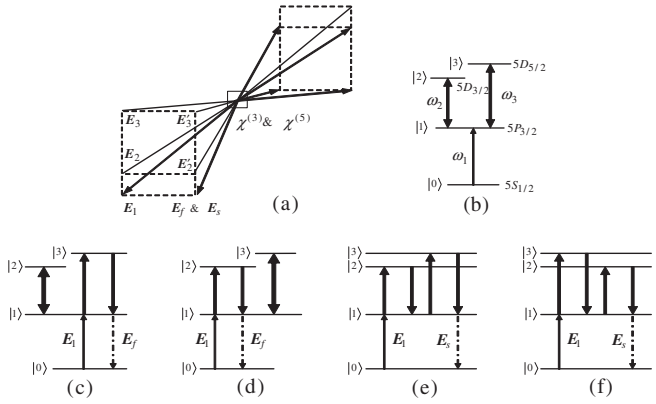

FIG. 1. (a) Spatial beam geometry used in the experiment. (b) Simple Y-type atomic system with dual ladder-type EIT. (c),(d) FWM processes with two pump beams in one upper transition dressed by a strong coupling beam in another upper transition. (e),(f) SWM processes with two pump beams in one upper transition and two photons from the coupling beam from another upper transition. $\boldsymbol{E}_f$ and $\boldsymbol{E}_s$ (dash-dotted lines) are the generated FWM and SWM signals, respectively. The bold double heading arrows imply the strong coupling beam.

drives the transition $|1\rangle$ to $|2\rangle$, as shown in Fig. 1(c), there will be multiwave-mixing processes that generate signal fields at frequency ω_1. First, without the strong field E_2, a simple FWM process (the probe beam E_1 and two pump fields E_3 and E_3') will generate a signal field $\boldsymbol{E}_f$ at frequency ω_1 via the perturbation chain (I) $\rho_{00}^{(0)} \xrightarrow{\omega_1} \rho_{10}^{(1)} \xrightarrow{\omega_3} \rho_{30}^{(2)} \xrightarrow{-\omega_3} \rho_{10}^{(3)}$. When the coupling field E_2 is turned on, it will dress the energy level $|1\rangle$ to create dressed states $|+\rangle$ and $|-\rangle$, and dressed-state FWM processes will occur as studied theoretically in various multilevel atomic systems [11]. Other than the FWM processes, there are also possible SWM processes as shown in Figs. 1(e) and 1(f) in this system, where two photons from E_2 and one photon each from E_3 and E_3' participate in the SWM processes to generate $\boldsymbol{E}_s$. These FWM and SWM processes can exist at the same time and can be phase matched to travel in the same direction. Similarly, when two pump fields, E_2 and E_2' (ω_2, $\mathbf{k}_2'$, and Rabi frequency G_2'), are used to drive the transition $|1\rangle$ to $|2\rangle$ and one strong coupling field E_3 drives the transition $|1\rangle$ to $|3\rangle$, as shown in Fig. 1(d), there will be similar FWM and SWM processes.

The pump and coupling laser beams are aligned spatially in the pattern as shown in Fig. 1(a), with four pump and coupling beams (E_2, E_2', E_3, E_3') propagating through the atomic medium in the same direction with small angles ($\sim 0.3°$) between them in a square-box pattern. During our experiment, one of the pump beams (E_2') is always blocked so we will only consider the system shown in Fig. 1(c). The probe beam (E_1) propagates in the opposite direction with an angle as shown in Fig. 1(a). Since the angles between the propagation directions are very small, this configuration satisfies the two-photon Doppler-free conditions for the two ladder-type EIT subsystems [7]. For simplicity, we will only consider the diffracted FWM and SWM signals relevant to our experimental measurements. By setting the propagation direction of the probe beam E_1 as indicated in Fig. 1(a) and blocking E_2', the diffracted FWM ($\boldsymbol{E}_f$) and SWM ($\boldsymbol{E}_s$) signal beams will be in the same direction determined by the phase-matching conditions: $\mathbf{k}_f = \mathbf{k}_1 + \mathbf{k}_3 - \mathbf{k}_3'$ and $\mathbf{k}_s = \mathbf{k}_1 + \mathbf{k}_2 - \mathbf{k}_2 + \mathbf{k}_3 - \mathbf{k}_3'$, respectively. The total FWM process can be considered as due to the constructive or destructive interference between the two dressed FWM channels. We can write down the two SWM processes [indicated in Figs. 1(e) and 1(f)] as (II) $\rho_{00}^{(0)} \xrightarrow{\omega_1} \rho_{10}^{(1)} \xrightarrow{\omega_2} \rho_{20}^{(2)} \xrightarrow{-\omega_2} \rho_{10}^{(3)} \xrightarrow{\omega_3} \rho_{30}^{(4)} \xrightarrow{-\omega_3} \rho_{10}^{(5)}$ and (III) $\rho_{00}^{(0)} \xrightarrow{\omega_1} \rho_{10}^{(1)} \xrightarrow{\omega_3} \rho_{30}^{(2)} \xrightarrow{-\omega_3} \rho_{10}^{(3)} \xrightarrow{\omega_2} \rho_{20}^{(4)} \xrightarrow{-\omega_2} \rho_{10}^{(5)}$, respectively.

In general for arbitrary field strengths of E_2, E_3, and E_3', one needs to solve the 11 coupled density-matrix equations to higher orders to obtain $\rho_{10}^{(3)}$ for the FWM and $\rho_{10}^{(5)}$ for the SWM processes, which we have done in simulating the experimental results later on. In order to see the relation and interplay between these FWM and SWM processes, we calculate these nonlinear susceptibilities via appropriate perturbation chains here for simplicity. When both E_2 and E_2' are blocked, the simple FWM via chain (I) gives $\rho_{10}^{(3)} = -iG_a e^{i\mathbf{k}_f\cdot\mathbf{r}}/(d_1^2 d_3)$, where $G_a = G_1 G_3 (G_3')^*$, $d_1 = \Gamma_{10} + i\Delta_1$, $d_3 = \Gamma_{30} + i(\Delta_1 + \Delta_3)$ with $\Delta_i = \Omega_i - \omega_i$, and Γ_{ij} is the transverse relaxation rate between states $|i\rangle$ and $|j\rangle$. Next, when the coupling field E_2 is turned on, the above simple FWM process will be dressed and a perturbative approach for such interaction can be described by the following coupled equations:

$$\partial\rho_{10}^{(1)}/\partial t = -d_1\rho_{10}^{(1)} + iG_1 e^{i\mathbf{k}_1\cdot\mathbf{r}}\rho_{00}^{(0)} + iG_2^* e^{-i\mathbf{k}_2\cdot\mathbf{r}}\rho_{20} \quad \text{and} \quad \partial\rho_{20}/\partial t = -d_2\rho_{20} + iG_2 e^{i\mathbf{k}_2\cdot\mathbf{r}}\rho_{10}^{(1)}, \tag{1}$$

$$\partial\rho_{10}^{(3)}/\partial t = -d_1\rho_{10}^{(3)} + iG_2^* e^{-i\mathbf{k}_2\cdot\mathbf{r}}\rho_{20} + iG_3'^* e^{-i\mathbf{k}_3\cdot\mathbf{r}}\rho_{30}^{(2)} \quad \text{and} \quad \partial\rho_{20}/\partial t = -d_2\rho_{20} + iG_2 e^{i\mathbf{k}_2\cdot\mathbf{r}}\rho_{10}^{(3)}, \tag{2}$$

where $d_2 = \Gamma_{20} + i(\Delta_1 + \Delta_2)$. Equations (1) and (2) ($\rho_{00}^{(0)} \approx 1$) can be solved together with chain (I) to give $\rho_{10}' = -2iG_a e^{i\mathbf{k}_f\cdot\mathbf{r}} d_2/[d_1 d_3 (d_1 d_2 + |G_2|^2)]$.

Expression ρ_{10}' shows an interesting interplay between the FWM and SWM processes [16]. With coupling field E_2 on, the intermediate energy level $|1\rangle$ is dressed to become two split levels $|+\rangle$ and $|-\rangle$ with induced coherence between them. The FWM signals will have quantum interference via these two different split intermediate levels $|+\rangle$ and $|-\rangle$, which can either enhance or suppress the total observed FWM signal. When the coupling field G_2 is very strong [$G_2 \gg G_3(G_3') \gg G_1$], there exists a maximum suppression of the FWM at the condition $\Delta_1 = -\Delta_2 = -\Delta_3$. Also, one can easily calculate the susceptibility $\rho_{10}^{(5)}$ for SWM from pathways (II) and (III) [as shown in

Figs. 1(e) and 1(f)] directly to be $\rho_{10}^{(5)} = \rho_{10}^{(\mathrm{II})} + \rho_{10}^{(\mathrm{III})} = 2iG_a|G_2|^2 e^{i\mathbf{k}_s\cdot\mathbf{r}}/(d_1^3 d_2 d_3)$.

The two EIT windows are generated by the double-ladder EIT subsystems in the Y-type four-level system with both pump fields (between $|1\rangle$ and $|3\rangle$) and coupling field (between $|1\rangle$ and $|2\rangle$) stronger than the probe beam (between $|0\rangle$ and $|1\rangle$), as shown in Fig. 1(c). Since the generated SWM signal falls into one ladder-type EIT window ($|0\rangle - |1\rangle - |2\rangle$ branch), the SWM processes can be very efficient, especially when the FWM signal is suppressed. For finite frequency detunings Δ_2 and Δ_3, the two EIT windows in the Y-type system will be separated, and the generated FWM and SWM signals in these two EIT windows are easily distinguishable. There is one three-photon interference pathway (i.e., interference between $\omega_1 + \omega_3 - \omega_3$ and ω_1) for the FWM process and two five-photon interference pathways (i.e., between five-photon $\omega_1 + \omega_2 - \omega_2 + \omega_3 - \omega_3$ and ω_1, and between five-photon $\omega_1 + \omega_3 - \omega_3 + \omega_2 - \omega_2$ and ω_1) for the SWM processes. In this system, the three-photon and five-photon interferences are destructive ones, in which $\chi^{(3)}$ and $\chi^{(5)}$ are zeros at the line centers. Coexisting SWM and FWM signal efficiencies and the amount of suppression of the FWM signal are most prominent under the multiple-EIT condition of $\Delta_1 = -\Delta_2 = -\Delta_3$ and $G_2 \gg G_3(G_3') \gg G_1$ in Fig. 1(c) [and $G_3 \gg G_2(G_2') \gg G_1$ in Fig. 1(d)].

The experimental demonstrations of coexisting FWM and SWM processes, as well as controllable FWM and SWM processes, were carried out in atomic vapor of ^{87}Rb. The energy levels of $5s_{1/2}(F = 2)$, $5p_{3/2}$, $5d_{3/2}$, and $5d_{5/2}$ form the four-level Y-type system as shown in Fig. 1(b). The laser beams were carefully aligned as indicated in Fig. 1(a) (without E_2'). The vapor cell temperature is set at 60 °C. The probe laser beam E_1 [with wavelength of 780 nm from an external cavity diode laser (ECDL), connecting transition $5s_{1/2} - 5p_{3/2}$] is horizontally polarized and has a power of about $P_1 \approx 3.5$ mW. The pump laser beams E_3 and E_3' (wavelength 775.98 nm connecting transition $5p_{3/2} - 5d_{5/2}$) are split from a cw Ti:sapphire laser with equal power ($P_3 \approx P_3'$), each with a vertical polarization. The coupling laser beam E_2 (with power P_2, and wavelength 776.16 nm connecting transition $5p_{3/2} - 5d_{3/2}$) is from another ECDL and is vertically polarized. Great care was taken in aligning the laser beams with spatial overlaps and wave vector phase-matching conditions with small angles (~0.3°) between them. The diameters at the vapor cell center for the pump and coupling beams are about 0.5 mm, respectively, and the diameter of the probe beam (E_1) is about 0.3 mm. The diffracted FWM and SWM signals ($\mathbf{k}_f$ and $\mathbf{k}_s$) with horizontal polarization are in the direction of $\boldsymbol{E}_f$ and $\boldsymbol{E}_s$ [at the lower right-hand corner of Fig. 1(a)] and are detected by an avalanche photodiode detector (APD). The transmitted probe beam is simultaneously detected by a silicon photodiode.

The dual-EIT windows of the Y-type system are measured by setting the frequency detunings at $\Delta_2 = -112$ MHz and $\Delta_3 = 0$, with three laser beams (E_2, E_3, and E_3') on. These two modified EIT windows from the two ladder-type EIT subsystems (at $\Delta_1 = -\Delta_2$ and $\Delta_1 = -\Delta_3$ EIT positions in probe transmission trace) are depicted in Fig. 2 [peaks 4 and 5 of curve (b)]. Meanwhile, as the probe detuning Δ_1 is scanned, several generated wave-mixing signals are observed on the APD [curve (a) of Fig. 2]. We identify peak 2 as a combination of the FWM signal ($\mathbf{k}_f$) and a small amount of SWM signal ($\mathbf{k}_s$). Peak 3 is the SWM signal ($\mathbf{k}_s$) and peak 1 is another FWM signal ($\mathbf{k}_f$) outside the EIT windows. Since the FWM and SWM signals are diffracted in the same spatial direction, we identify them by selectively blocking different laser beams and detuning different laser frequencies. We intentionally set large frequency detunings to separate the generated FWM and SWM signals in Fig. 2 for clarity. When the difference between Δ_2 and Δ_3 is reduced, these two EIT windows start to merge and the FWM and SWM signals begin to interfere. The dip in the middle of the FWM signal [peak 2 of curve (a) in Fig. 2] is due to three-photon destructive interference.

Figure 3(a) shows the FWM signal as a function of coupling power P_2, corresponding to peak 2 in Fig. 2. The top curve is for $P_2 = 0$, which is a simple FWM signal. The dip in the middle is due to three-photon destructive interference. As the coupling field E_2 is turned on, SWM signals within EIT windows (in peak 2 and peak 3 in Fig. 2) start to emerge and increase as P_2 increases. Such increases of SWM signals are at the cost of the FWM process. As shown in Figs. 3(a) and 3(b), as P_2 increases, the FWM signal decreases substantially (about 3 times in the P_2 power range shown) due to the destructive interference between two dressed FWM channels. In such a way, the relative strengths between FWM and SWM signals in the two EIT windows can be adjusted by simply tuning the coupling beam power P_2, which is very important for the

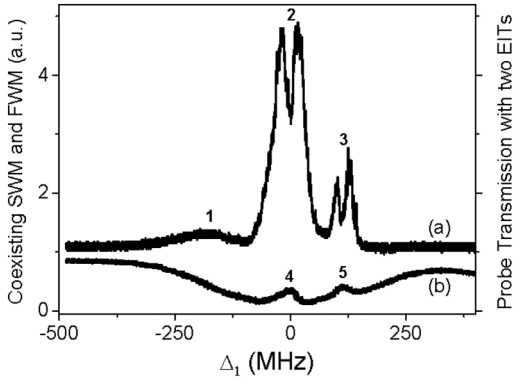

FIG. 2. Curve (a): Measured SWM (peak 3) and FWM (peaks 1 and 2) signals. Curve (b): Probe beam transmission (peaks 4 and 5: two ladder-type EIT windows) versus the probe detuning Δ_1. The experimental parameters are $P_1 = 3.6$ mW, $P_2' = 0$, $P_2 = 33$ mW, $P_3 = P_3' = 130$ mW, $\Delta_2 = -112$ MHz, and $\Delta_3 = 0$.

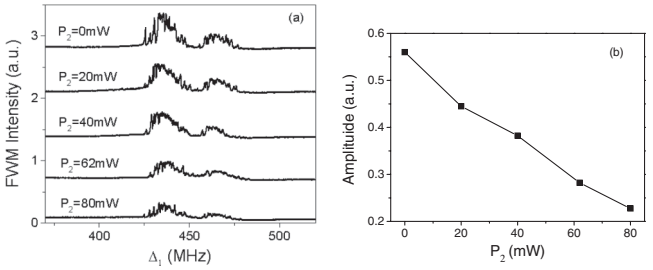

FIG. 3. (a) Measured FWM signal intensity for various coupling field powers versus the probe detuning Δ_1. (b) FWM amplitude versus the ω_2 coupling field power. $P_1 = 3.4$ mW, $P_2' = 0$, $P_2 = 0$, 20, 40, 62, 80 mW, $P_3 = 34$ mW, $P_3' = 17$ mW, $\Delta_2 = -200$ MHz, and $\Delta_3 = -450$ MHz.

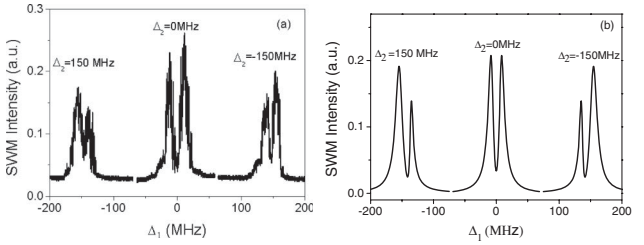

FIG. 4. (a) Measured SWM signal spectra for different coupling field E_2 frequencies. (b) Theoretical plot of SWM intensity versus Δ_1 for different Δ_2 values. $P_1 = 3.4$ mW, $P_2' = 0$, $P_2 = 34$ mW, $P_3 = P_3' = 96$ mW, $\Gamma_{10}/2\pi = 3$ MHz, $\Gamma_{20} = \Gamma_{30} = 2\pi \times 0.5$ MHz, $\Delta_3 = -450$ MHz, and $\Delta_2 = -150$, 0, 150 MHz.

interplay and control between FWM and SWM processes in this system. Maximal enhancement of SWM signal and the largest suppression of FWM signal can be achieved at the multi-EIT condition of $\Delta_1 = -\Delta_2 = -\Delta_3$ with a large value of P_2.

Figure 4 presents the changes of the SWM signal (corresponding to peak 3 in Fig. 2) as a function of the coupling field frequency detuning. It is seen from Fig. 4(a) that, as the coupling frequency detuning Δ_2 changes, the generated SWM signal changes from symmetric to asymmetric, which is due to two-photon [7] or three-photon [10] resonant emission enhancement. Such asymmetric SWM spectra have been simulated by numerically solving the 11 coupled density-matrix equations for the system at the steady state and are plotted in Fig. 4(b). The dips at the line center of the SWM spectra are due to five-photon (one probe photon plus four pump and coupling photons) destructive interference with the generated signal photon, which looks like a multiphoton EIT phenomenon but is actually a suppression of generating SWM due to multiphoton destructive interference at the exact resonance.

The maximal FWM and SWM efficiencies in this system are quite high (measured to be about 10% and 1%, respectively). The coexistence of these two nonlinear wave-mixing processes in this system can be used to evaluate the high-order nonlinear susceptibility $\chi^{(5)}$ by beating the FWM and SWM signals. This four-level atomic system with coexisting FWM and SWM consists of three conventional two-photon Doppler-free EIT subsystems, i.e., $|0\rangle - |1\rangle - |2\rangle$ (ladder type), $|0\rangle - |1\rangle - |3\rangle$ (ladder type), and $|2\rangle - |1\rangle - |3\rangle$ (V type). In general, we can investigate interesting interplays between two fundamental nonlinear wave-mixing processes and identify ways to enhance the higher-order nonlinear optical processes through opening new nonlinear channels via atomic coherence and quantum interference.

In conclusion, we have demonstrated highly efficient dual-EIT-assisted (or opened) FWM and SWM processes in the four-level Y-type atomic system due to atomic coherence and quantum interference. The coexistence and competition between these two nonlinear optical wave-mixing processes in this open-cycle atomic system are quite different from the previously studied independent FWM and SWM processes. We observed suppression and enhancement of the FWM signals resulting from destructive and constructive interferences via the two dressed FWM channels. Three-photon and five-photon destructive interferences are clearly observed in the generated coherent FWM and SWM signals, respectively. Understanding and optimizing higher-order nonlinear optical processes can have important applications in many areas of physics.

We acknowledge funding support from the National Science Foundation.

*ypzhang@mail.xjtu.edu.cn
†mxiao@uark.edu.

[1] P. R. Hemmer *et al.*, Opt. Lett. **20**, 982 (1995).
[2] Y. Li and M. Xiao, Opt. Lett. **21**, 1064 (1996).
[3] M. M. Kash *et al.*, Phys. Rev. Lett. **82**, 5229 (1999).
[4] D. A. Braje *et al.*, Phys. Rev. Lett. **93**, 183601 (2004).
[5] H. Kang *et al.*, Phys. Rev. A **70**, 061804 (2004).
[6] S. E. Harris, Phys. Today **50**, No. 7, 36 (1997).
[7] J. Gea-Banacloche *et al.*, Phys. Rev. A **51**, 576 (1995).
[8] H. Kang *et al.*, Phys. Rev. Lett. **93**, 073601 (2004).
[9] G. S. Agarwal and W. Harshawardhan, Phys. Rev. Lett. **77**, 1039 (1996).
[10] A. S. Zibrov *et al.*, Phys. Rev. A **65**, 043817 (2002).
[11] L. Deng and M. G. Payne, Phys. Rev. Lett. **91**, 243902 (2003).
[12] C. Hang *et al.*, Phys. Rev. A **74**, 012319 (2006).
[13] H. Michinel *et al.*, Phys. Rev. Lett. **96**, 023903 (2006).
[14] H. Ma and C. B. de Araujo, Phys. Rev. Lett. **71**, 3649 (1993).
[15] J. B. Qi *et al.*, Phys. Rev. Lett. **83**, 288 (1999).
[16] Y. P. Zhang and M. Xiao, Appl. Phys. Lett. **90**, 111104 (2007).